

# Gas antisolvent fractionation of semicrystalline and amorphous poly(lactic acid) using compressed CO<sub>2</sub>

Geoffrey D. Bothun, Karen L. White<sup>1</sup>, Barbara L. Knutson\*

*Department of Chemical and Materials Engineering, University of Kentucky, Lexington, KY 40506-0046, USA*

Received 5 September 2001; received in revised form 1 March 2002; accepted 4 March 2002

## Abstract

Semicrystalline and amorphous poly(lactic acid) (L-PLA and D,L-PLA, respectively) were fractionated from chloroform solutions using compressed CO<sub>2</sub> as an antisolvent. The following process variables were used to precipitate normalized molecular weight fractions (NMW) of L-PLA ranging from 0.81 to 1.54 relative to the starting material: polymer concentration, initial organic solution volume, and the rate of antisolvent addition. An analysis of variance (ANOVA) used to quantify the importance of these variables determined that polymer concentration had the most significant impact on the NMW of L-PLA precipitated in this gas antisolvent (GAS) precipitation process. The results of the ANOVA also suggest a predictive approach to polymer fractionation in this complex system. The analysis also highlights the differences and similarities between the fractionation of semicrystalline and amorphous polymers using compressed antisolvents. © 2002 Elsevier Science Ltd. All rights reserved.

*Keywords:* Gas antisolvent precipitation; Polymer fractionation; Compressed antisolvent

## 1. Introduction

Supercritical or near-supercritical fluids (SCF) have gained increasing interest as antisolvents for the generation of ultrafine particles and the separation of dissolved solutes. Gas antisolvent recrystallization (GAS) and other precipitation processes based on compressed antisolvents have been employed to produce sub-micron particles of superconductor precursors, pigments, explosives, and a variety of pharmaceuticals for controlled drug release applications [1–3]. Precipitation is achieved by contacting an organic solution containing the dissolved solute with a solvent-miscible compressed antisolvent. This results in a volume expansion of the organic solution and reduction of solvent strength, subsequently precipitating the solute. The advantages of using compressed antisolvents are the ability to recover a solvent-free product following depressurization, solute precipitation at relatively moderate pressure (<100 bar), and its applicability to thermally labile compounds. The most common compressed antisolvent employed is CO<sub>2</sub> ( $T_c = 31.1$  °C,  $P_c = 73.8$  bar), which is environmentally benign, non-toxic, relatively inexpensive, and easily recovered following depressurization.

GAS recrystallization has been successfully applied to many processes that require high purity and narrow size distributions. The high supersaturations achieved in this rapid precipitation process are effective in controlling microparticle morphology, specifically size and size distribution, for a variety of compounds such as organic salts, pharmaceuticals, and polymeric materials [4–8]. GAS has also been explored as a means of separating small dissolved solutes, such as naphthalene and phenanthrene in toluene, using compressed CO<sub>2</sub> as the antisolvent [9–11]. GAS-based separations are achieved through the partial expansion of the dissolved organic solution by a compressed antisolvent, resulting in the selective precipitation of a solute as a function of solubility. For both the recrystallization and separation processes, the rate of antisolvent addition has been identified as an important parameter for controlling the microparticle morphology and selectivity of the separation, respectively [4,11–13].

More recently, GAS has been used to separate higher molecular weight compounds. The ability to purify or fractionate proteins has been demonstrated [14,15]. Similarly, the separation of lecithin and soy oil mixtures using GAS precipitation has been successfully performed by Catchpole et al. [16]. The pressure at which the mixed solutes precipitated from the gas-expanded solution did not correspond to the precipitation pressure of the individual solutes. Therefore, it was not possible to accurately predict

\* Corresponding author. Tel.: +1-859-257-5715; fax: +1-859-323-1929.  
E-mail addresses: bknutson@engr.uky.edu (K.L. White).

<sup>1</sup> Present address: Imation Corporation, Wahpeton, ND, USA.

separation based on the behavior of the individual solutes [16].

Tan and Chang [17] observed a reduction in the MW of polystyrene microparticles precipitated by GAS. Compressed HFC-134a, a fluorinated alkane, was used to partially expand a solution of dissolved polystyrene (185,000 MW) in chloroform (5–10 wt% polymer). The rate of volume expansion of the organic phase and the operating temperature were found to have the most significant influence on the MW of the precipitated particles. Partial GAS expansion processes are also capable of precipitating higher or lower MW fractions of poly(lactic acid) (PLA), depending on the process conditions [18]. The following process variables were investigated previously for the fractionation of PLA: rate of antisolvent addition, initial organic solution volume, and temperature. The interrelated kinetic and thermodynamic processes leading to precipitation of polymers by GAS suggests a complex relationship between process variables and fractionation.

Antisolvent precipitation is commonly described as a non-equilibrium, mass transfer limited process, therefore, pathways that are energetically favorable may be suppressed [19–21]. Antisolvent precipitation is particularly complicated when processing semicrystalline polymers, which can precipitate by either solid–liquid (S–L; crystallization) or liquid–liquid (L–L; liquid phase nucleation and growth or spinodal decomposition followed by a solidification step) demixing. Demixing in antisolvent membrane formation techniques using semicrystalline polymers is considered to be primarily dependent upon polymer concentration, with greater concentrations favoring S–L demixing [19,20,26]. At intermediate polymer concentrations, pathways associated with either L–L or S–L demixing may develop, suggesting the possibility of influencing this behavior with GAS processing. While S–L demixing may be energetically or thermodynamically more favorable for a given composition, L–L demixing frequently dominates the precipitation process because it is kinetically more favorable [19].

The goal of this investigation is to demonstrate the fractionation of semicrystalline (L-PLA) and amorphous (D,L-PLA) poly(lactic acid) by GAS and to determine the influence of relevant GAS variables on fractionation through statistical analysis. FDA-approved L-PLA was selected for this investigation because of its application as a matrix in controlled drug release devices [3,22,23]. The release rate of a pharmaceutical agent from a biodegradable polymer matrix is controlled by the degradation rate of the polymer and/or diffusion of the drug through the matrix. The degradation and release rates are proportional to the polymer MW, suggesting the need for polymer synthesis and fractionation methods to tailor polymer MW and MW distribution. Previous studies have successfully employed GAS to produce sub-micron particles of both L-PLA and composites of polymers and pharmaceuticals [3,7]. A reduction in the MW of polystyrene microparticles

formed by GAS further suggests that simultaneous fractionation may be possible [17].

A design of experiment approach was used to identify the significance of the following GAS variables on fractionation: polymer concentration, initial solution volume, and antisolvent pressurization rate. The information gained from the factorial experimental design quantifies the physical significance of the GAS operating parameters and suggests the ability to predict the results of similar fractionations. Similarities and differences between the precipitation of semicrystalline and amorphous polymer fractionation by GAS are also described. In addition, the key variables governing fractionation for L-PLA and D,L-PLA are compared for the processing of semicrystalline and amorphous polymers of similar MW.

## 2. Materials and methods

### 2.1. Materials

Semicrystalline L-PLA (100,000 MW) was purchased from Polysciences Inc. and amorphous D,L-PLA (106,000 MW) was purchased from Sigma-Aldrich. The polydispersity of both L- and D,L-PLA was determined experimentally by gel permeation chromatography to be  $2.27 \pm 0.63$  and  $1.41 \pm 0.32$ , respectively. Chloroform (99.9%, Reagent Grade) and tetrahydrofuran (THF, certified spectranalyzed) from Fisher Scientific were used as solvents. High purity carbon dioxide gas (99.99%) was obtained from AGA speciality gas. All materials were used without further purification. The polymers were stored under refrigeration to inhibit degradation. Polystyrene calibration standards for the gel permeation chromatography analysis of the polymer MW were purchased from Polymer Standards Services- USA, Inc. The standards include 42, 112, 178, and 464 ( $\times 10^3$ ) MW samples of narrow polydispersity ( $PD < 1.03$ ).

### 2.2. Experimental methods

A Jerguson view cell (42 ml, rated to 345 bar) was used as the precipitation chamber (Fig. 1). Safety features of the view cell include a rupture disk rated to 345 bar, a physical enclosure containing a plexiglass window for viewing, and pressurised viewing windows positioned perpendicular to the observer. The level of organic solution expansion was visually monitored using a mirror located at an angle relative to the chamber windows. A syringe pump (ISCO model 500D) was used to supply compressed CO<sub>2</sub> to the chamber. The cell pressure and antisolvent pressurization rate were measured using a pressure gauge (Druck model DPI  $280 \pm 0.1$  bar) located at the top of the view cell. The antisolvent flowrate and system pressure were maintained using a stainless steel micrometering valve (Autoclave model 10VRMM2812). A stainless steel vessel (150 ml Whitey, rated to 124 bar) was used as an expansion vessel for depressurization. Precipitate formed in the chamber was collected

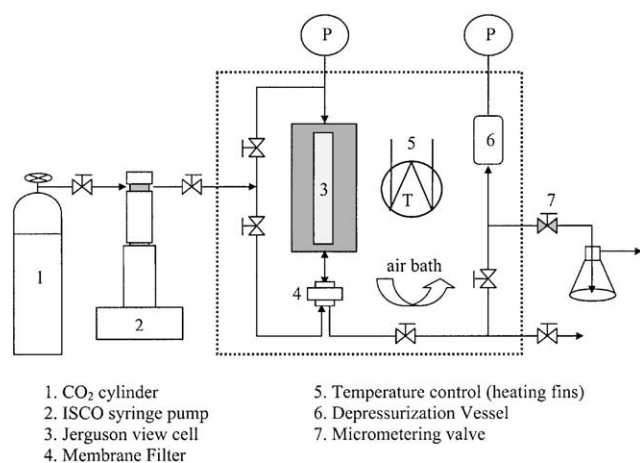


Fig. 1. Schematic of the GAS experimental apparatus. The perforated boundary (line) indicates a physical enclosure for safety purposes and to insulate for isothermal operation.

by forcing the CO<sub>2</sub>-expanded organic phase through a 0.2 μm nylon membrane Millipore® filter located at the bottom of the chamber.

Solutions for fractionation were prepared by dissolving PLA in chloroform at ambient temperatures and stirring until dissolved. The samples were stored for roughly 24 h to insure dissolution and chain relaxation. The precipitation chamber was heated in a circulating air bath to 45 °C at ambient pressure for temperature equilibration and to drive off moisture. The chamber was then charged with a known volume of the polymer solution at atmospheric pressure and sealed. CO<sub>2</sub> was introduced into the chamber by bubbling through the bottom of the view cell at a pre-determined pressurization rate.

Addition of the CO<sub>2</sub> resulted in an expansion of the solvent phase that was measured visually in the precipitation chamber. The pressure (due to antisolvent addition) at which the expanded organic solution became clouded with solid precipitant was recorded as the cloud point pressure,  $P_{CP}$ . The vessel was allowed to equilibrate at the pressure at which the polymer precipitated until precipitation ceased (visually observed). While maintaining  $P_{CP}$ , the flow of CO<sub>2</sub> was reversed and the contents of the cell were forced through the filter located at the bottom of the cell. The precipitated polymer was collected on the filter, and the chloroform was recovered at atmospheric pressure in a sample vial.

Following filtration, the processed polymer was further dried for approximately 1 h with 6 ml/min of CO<sub>2</sub> at the precipitation pressure and operating temperature ( $P_{CP}$  and 45 °C) to remove residual solvent. The system was then depressurized over 30 min. The membrane filter was removed and stored in a desiccator until analysis.

### 2.3. Analysis of the polymer MW

The molecular weight of the precipitated PLA samples

was determined using a gel permeation chromatograph (Waters® 150C GPC) equipped with a refractive index detector. A Styragel® HT4 column packed with 5 μm styrene divinylbenzene particles (dimensions, 7.8 × 300 mm<sup>2</sup>; MW range, 5000–600,000) was used with a THF flowrate of 1 ml/min.

Solid PLA samples collected on the membrane filter were solubilized in THF by immersing the membrane in a sealed vial, and placing it in a 50–60 °C water bath for 1 h. The solutions were then allowed to equilibrate overnight at room temperature to ensure relaxation of the polymer chains. Prior to analysis, the samples were filtered through a 0.45 μm poly(tetrafluoroethylene) syringe filter. The samples were then placed into sealed sample vials and equilibrated to 40 °C, the operating temperature of the GPC.

A MW calibration curve was constructed using 42, 112, 178, and 464 (× 10<sup>3</sup>) MW polystyrene standards. Each PS standard was analyzed via GPC in triplicate and the average time of elution of the maximum peak height was used to construct the calibration curve for determining PLA MW. A new calibration curve was constructed each day the PLA samples were analyzed.

The weight-averaged MW was calculated according to the following equation:

$$MW_w = \frac{\sum_i c_i MW_i^2}{\sum_i c_i MW_i} \quad (1)$$

where  $c_i$  is the concentration of the  $i$ th component with molecular weight  $MW_i$ . The MW of both the processed and unprocessed polymer were analyzed concurrently to account for variations in the instrument and possible PLA biodegradation of the starting material due to hydrolysis. The extent of fractionation is expressed in terms of a normalized weight average molecular weight ( $NMW = MW_{\text{processed}}/MW_{\text{unprocessed}}$ ).  $NMW > 1$  indicates the precipitation of a higher MW fraction relative to the starting (unprocessed) material and  $NMW < 1$  indicates the precipitation of a lower MW fraction. Standard deviations for processed L-PLA fractionation experiments are based on duplicate experiments and multiple GPC analysis. The standard deviations reported for processed D,L-PLA are the result of multiple GPC analysis.

### 2.4. Design of experiment and statistical analysis

Due to the large number of possible independent variables associated with the GAS process, a factorial design approach was used to determine the influence of key parameters and parameter interactions based on a minimum number of L-PLA fractionation experiments. The effects of polymer concentration (3 and 8 mg/ml), initial polymer-organic solution volume (5 and 10 ml) in the precipitation chamber, and rate of CO<sub>2</sub> addition (or pressurization rate, 0.41 and 1.38 bar/min) were analyzed.

Table 1

Experimental conditions (polymer concentration, initial solution volume, and CO<sub>2</sub> pressurization rate) and results ( $P_{CP}$  and NMW) for the GAS fractionation of L- and D,L-PLA in chloroform with compressed CO<sub>2</sub>

Experiment no.	Polymer concentration (mg/ml)	CO <sub>2</sub> pressurization rate (bar/min)	Initial organic solution volume (ml)	Cloud point pressure, $P_{CP}$ (bar)	Normalized MW (NMW)
<i>L-PLA–chloroform–CO<sub>2</sub></i> <sup>a</sup>					
1	3	0.41	5	62.8	0.81 ± 0.14
2	3	1.38	5	63.4	0.89 ± 0.08
3	3	0.41	10	63.8	1.02 ± 0.02
4	3	1.38	10	65.5	1.05 ± 0.11
5	8	0.41	5	63.2	1.44 ± 0.17
6	8	1.38	5	63.8	1.52
7	8	0.41	10	65.4	1.43
8	8	1.38	10	67.6	1.54 ± 0.03
<i>D,L-PLA–chloroform–CO<sub>2</sub></i> <sup>b</sup>					
9	3	0.41	5	64.8	1.46 ± 0.01
10	3	1.38	5	65.1	1.39 ± 0.21
11	8	0.41	5	64.3	1.55
12	8	1.38	5	62.2	1.7 ± 0.05

<sup>a</sup> Standard deviation based on multiple experiments and GPC analyses.

<sup>b</sup> Standard deviation based on multiple GPC analyses.

The fractionation of relatively dilute concentrations (3 and 8 mg/ml; 0.2 and 0.54 wt%, respectively) of the semicrystalline and amorphous polymers were investigated at constant temperature (45 °C). This concentration range was chosen to represent the range employed in typical compressed antisolvent precipitation experiments [3] and to ensure minimal chain overlap in solution [24].

A factorial design of experiment with three parameters requires 2<sup>*n*</sup> experimental runs, where *n* is equal to the number of individual variables tested (*n* = 3, L-PLA; *n* = 2, D,L-PLA). The conditions for each experiment are provided in Table 1. An analysis of variance (ANOVA) was performed for both the L- and D,L-PLA fractionation to determine the magnitude of effect associated with each variable, and the cross-effects between potentially ‘coupled’ or interacting variables. NMW was related to the variables in the following polynomial form:

$$y = \beta_0 + \sum_{i=1}^n \beta_i x_i + \sum_i \sum_j \beta_{ij} x_i x_j \quad \text{where } i < j \quad (2)$$

where *y* represents the dependent variable NMW, *x<sub>i</sub>* the main effects or independent process variables, *x<sub>i</sub>x<sub>j</sub>* the cross-effects between independent variables, and the β’s are constants associated with each term. The relevance of each term associated with variable(s) *x<sub>i</sub>* and/or *x<sub>j</sub>* was examined based on the probability that the constant associated with each term is non-zero. This confidence was expressed in terms of the *F*-ratio (*F<sub>0</sub>*), which is determined by dividing the mean square for each source (variable) by the mean-square error for the specific system (model). Experimental *F*-ratios were compared to tabulated values (*F<sub>tab</sub>*) that are based on the desired confidence limit, and the degrees of freedom associated with the numerator and denominator

[25]. A probability of greater than 95% that the parameter β was non-zero was the criteria for accepting parameters in a stepwise regression scheme, as demonstrated by the *F*-ratio. Constructing the surface response plots for NMW (based on Eq. (2)) provides a basis for predicting the conditions necessary to achieve a desired GAS fractionation of L-PLA.

### 3. Results and discussion

The cloud point pressure ( $P_{CP}$ ) and the resulting NMW for the fractionation of L-PLA and D,L-PLA are given in Table 1 as a function of the fractionation conditions. Both polymers were successfully fractionated under the experimental conditions investigated. The ability to fractionate both high and low MW components of L-PLA using GAS precipitation was demonstrated. For example, increasing L-PLA concentration from 3 to 8 mg/ml while operating at the same CO<sub>2</sub> pressurization rate and initial solution volume results in an increase in NMW from 0.81 ± 0.14 to 1.44 ± 0.17 (experiments 1 and 5, respectively). The polydispersity of the processed PLA was not statistically different from unprocessed samples.

Increasing the polymer concentration, initial solution volume, and pressurization rate increases both  $P_{CP}$  and NMW for the fractionation of L-PLA.  $P_{CP}$  ranged from 62.8 to 67.6 bar corresponding to an increase in NMW from 0.81 ± 0.14 to 1.54 ± 0.03. Furthermore, L-PLA concentration has a significant effect on the NMW of the resulting precipitate. Increasing the initial solution concentration from 3 to 8 mg L-PLA/ml (0.2–0.54 wt%) increased processed NMW values by approximately 45% for all cases. Increasing the initial solution volume and CO<sub>2</sub> pressurization rate increased NMW by roughly 10%.

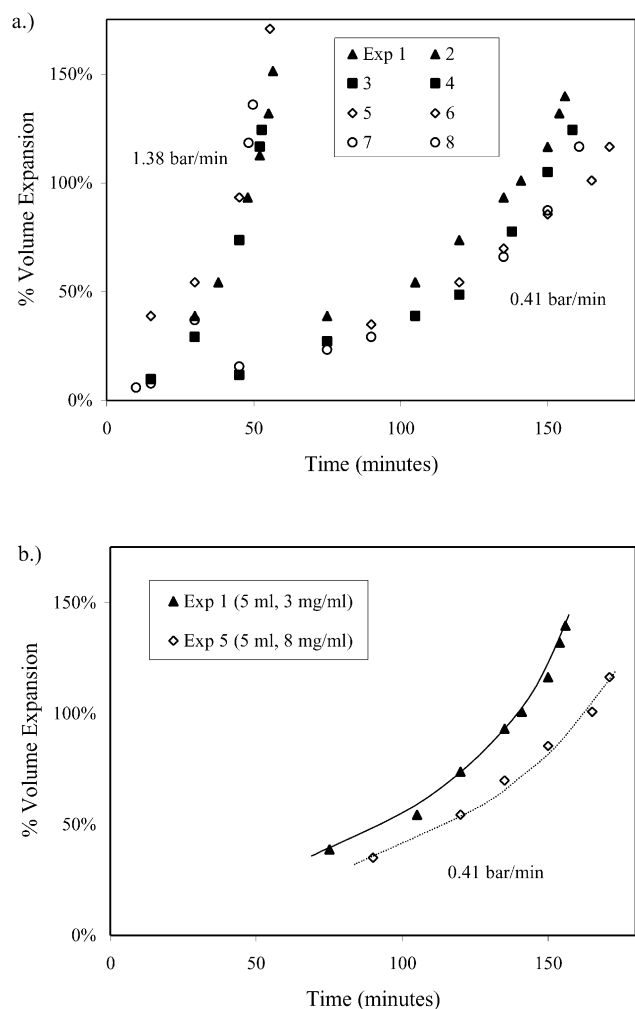


Fig. 2. Effect of L-PLA concentration (3 mg/ml, filled symbols; 8 mg/ml, unfilled symbols) on the organic phase volume expansion. (a) Plotted as a function of time for both CO<sub>2</sub> pressurization rates (0.41 and 1.38 bar/min) and (b) plotted as a function of time to represent the shift in expansion due to an increase in L-PLA concentration (experiments 1 and 5).

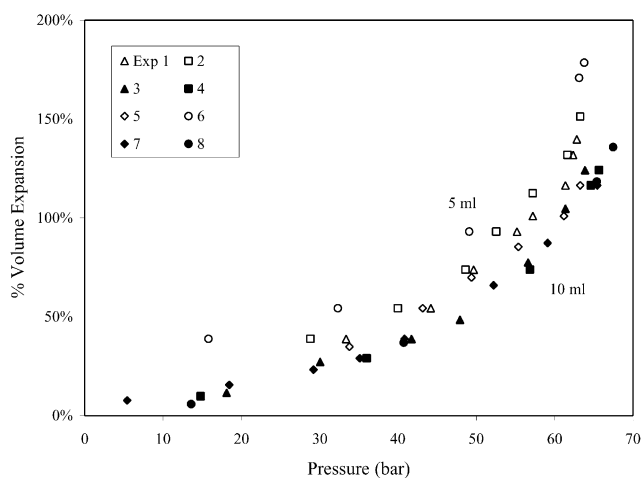


Fig. 3. Effect of L-PLA/chloroform initial solution volume on the volume expansion plotted as a function of total pressure. A shift in the volume expansion from 5 ml (unfilled symbols) to 10 ml (filled symbols) is shown.

### 3.1. Volume expansion of the organic solution

The volume expansion of the organic phase as a function of time (Fig. 2) is primarily governed by the rate of CO<sub>2</sub> pressurization. As expected, a pressurization rate of 1.38 bar/min results in a greater rate of expansion when compared to a pressurization rate of 0.41 bar/min. No significant differences in the volume expansion as a function of polymer concentration or initial solution volume were observed at the higher pressurization rate. However, at the lower pressurization rate there is a decrease in the rate of expansion as the L-PLA concentration increases from 3 to 8 mg/ml for the experiments conducted with 5 ml of initial solution volume (Fig. 2(b)). A decrease in the rate of volume expansion may be explained by a reduction in the rate of antisolvent diffusion into the solution due to an increase in viscosity. This trend is not evident in the low pressurization rate experiments conducted at higher initial solution volumes (10 ml).

Increasing the initial L-PLA/chloroform solution volume from 5 to 10 ml decreases the % volume expansion of the organic solution (defined as the change in solution volume in the presence of CO<sub>2</sub> relative to the initial solution volume) as a function of system pressure (Fig. 3). Initial solution volume would not affect the % volume expansion if CO<sub>2</sub> was uniformly distributed throughout the solution. Thus, the effect of solution volume on the expansion is further evidence of mass transfer limitations in the GAS process. The initial solution volume can be used to control the rate of CO<sub>2</sub> mass transfer into the organic solution, influencing the expansion behavior, and ultimately the precipitation conditions.

### 3.2. Precipitation pressure

The precipitation pressure ( $P_{CP}$ ) is also affected by polymer concentration, initial solution volume, and CO<sub>2</sub> pressurization rate (Table 1).  $P_{CP}$  is a physical measurement of CO<sub>2</sub> in the system at the time of precipitation. The  $P_{CP}$  associated with L-PLA fractionation increased with increasing initial solution volume, CO<sub>2</sub> pressurization rate, and most significantly, polymer concentration. A linear relationship exists between NMW and  $P_{CP}$  for L-PLA fractionation at 3 mg/ml L-PLA, and this relationship is nearly independent of solution volume and CO<sub>2</sub> pressurization (significant at 95% confidence;  $R^2 = 0.74$ ).

### 3.3. Analysis of the variance (ANOVA statistical analysis)

The effect of polymer concentration, initial polymer-organic solution volume, and CO<sub>2</sub> pressurization rate on the NMW of fractionated L-PLA was quantified by an ANOVA through a least squares stepwise regression. The results of the ANOVA analysis are presented in Table 2, which contains the significant effects, cross-effects, and the magnitude of these effects within 95% confidence limits. The fractionation of L-PLA is primarily dependent upon

Table 2  
Response surface based on ANOVA results for GAS fractionation of L-PLA

Source of variation	Sum of squares	F-value ( $F_0$ ) <sup>a</sup>	$\beta$ coefficients
Polymer concentration	0.1298	226.9	0.1611
Initial solution volume	0.0286	49.3	0.0578
Concentration $\times$ volume	0.0158	27.3	-0.0071
CO <sub>2</sub> pressurization rate	0.0114	19.7	0.0054
Model error	$6.0 \times 10^{-3}$		

<sup>a</sup> Significant at 95% confidence limits ( $F_0 > F_{\text{tab}}$ );  $F_{0.05,1,3} = 9.12$ .

the polymer concentration of the organic phase, as shown in Table 2. The effects of initial organic solution volume and pressurization rate are significant but secondary to concentration. In addition, the cross-effect between polymer concentration and initial solution volume suggest that a simultaneous increase in both variables results in the greatest NMW.

Our previous investigation of L-PLA fractionation on the GAS variables of initial organic solution volume (5 and 10 ml), CO<sub>2</sub> pressurization rate (0.41 and 1.38 bar/min), and system temperature (25 and 45 °C) at a constant polymer concentration (<1 wt%) [18]. Pressurization rate was the dominant variable in the fractionation of semicrystalline and amorphous PLA, although cross-effects between temperature and pressure were evident in the fractionation of L-PLA. For example, a higher temperature coupled with a faster pressurization rate or a lower temperature coupled with a slower pressurization rate resulted in an increase in the NMW of precipitated L-PLA. The predictability of the ANOVA was tested with additional L-PLA fractionation experiments. Although the general trends in L-PLA fractionation were predicted, the difference of these predictions exceeded that of the experimental uncertainty. In these previous experiments a low L-PLA concentration (8 mg/ml or 0.54 wt%) was investigated in an effort to reduce the influence of polymer concentration on demixing [24].

However, recent studies have shown that a change in the demixing or precipitation pressure for a polymer solution can occur at concentrations less than 1 wt% [21]. In addition, our previously observed ability (at constant polymer concentration) to fractionate either high or low MW polymer depending on GAS processing conditions [18] may be related to competing L–L and S–L demixing processes. At constant temperature, these physical processes are most closely related to the concentration of polymer in solution [16]. The strong dependence of fractionation on polymer concentration demonstrated in this work, and the ability to recover both high and low NMW polymers, suggest that the variables governing GAS precipitation affect the mechanism of demixing for this semicrystalline polymer.

The rate of antisolvent addition or pressurization rate is the focus of many GAS investigations and affects both volume expansion of the organic solvent and the extent of solute separation [4,11]. Mass transfer limitations in GAS

precipitation clearly lead to non-equilibrium conditions. These limitations are a function of pressurization rate, interfacial contact area between antisolvent and solution, and solution properties affecting diffusion, such as viscosity. This study suggests that the rate of volume expansion is sensitive to process variables and affects polymer fractionation. However, polymer concentration proves to be the most dominant parameter governing fractionation at constant temperature, challenging the notion that the antisolvent pressure or pressurization rate is the tunable parameter primarily responsible for achieving a selective separation. Our previous work [18] demonstrated that sequential, or stepwise, fractionations could be performed to achieve various molecular weight ranges of processed L-PLA samples using GAS precipitation at constant temperature (25 °C). Stepwise fractionations result in solutions of variable polymer concentration; therefore, further understanding of the effect of polymer concentration on fractionation by GAS is necessary.

A response surface that relates L-PLA fractionation (NMW) to the process variables was constructed using the coefficients of the significant terms ( $\beta$ ) determined by linear regression (Table 2). The response surfaces constructed in Fig. 4 represent the predicted conditions necessary to achieve L-PLA NMW fractions of 0.75, 1.0, 1.25, 1.5, and 2.0 in the precipitation chamber at 45 °C based on the range of variables investigated and the contacting scheme. For example, to obtain a processed weight-averaged MW that is 50% greater than the unprocessed L-PLA with 8 ml of solution, an L-PLA concentration of roughly 8 mg/ml and a pressurization rate ranging from 0.2 to 2 bar/min is required.

### 3.4. Fractionation of D,L-PLA

Amorphous PLA (D,L-PLA) of approximately the same

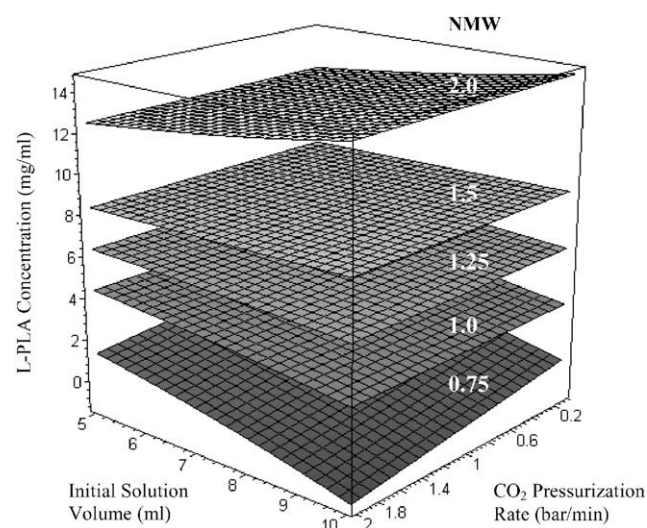


Fig. 4. NMW response surfaces for L-PLA fractionation based on ANOVA results ( $R^2 = 0.997$ ). Contours plotted as a function of L-PLA concentration, initial solution volume, and CO<sub>2</sub> pressurization rate. The labels on each surface represent the respective NMW.

MW as L-PLA was also fractionated to compare with results obtained for D,L-PLA. GAS fractionation produced only higher MW fractions (NMW > 1) of D,L-PLA over the range of conditions investigated (Table 1). In contrast, both high and low MW fractions of processed L-PLA were obtained. The effect of polymer concentration on the fractionation is similar for D,L-PLA and L-PLA; an increase in polymer concentration results in an increase in fractionated NMW. However, the NMW of the processed amorphous polymer decreased linearly as a function of  $P_{CP}$ , independent of D,L-PLA concentration and the CO<sub>2</sub> pressurization rate (linear regression at 95% confidence;  $R^2 = 0.93$ ). This is in contrast to the trend observed for the fractionation of L-PLA, where there was a positive correlation between NMW of the precipitated semicrystalline polymer and the pressure marking the onset of visual precipitation.

The low concentrations of semicrystalline polymer employed in this investigation would likely favor L–L demixing [19,20]. However, a comparison of the GAS fractionation of L- and D,L-PLA suggests that crystallization may play a role in the fractionation processes of semicrystalline polymers. Fractionation of D,L-PLA only yielded NMW greater than 1, while fractionation of L-PLA provided NMW greater than and or less than 1. The link between the NMW and the crystallinity of the processed semicrystalline polymer cannot be tested directly because of the potential for solvent-induced and CO<sub>2</sub>-induced crystallization of the polymer subsequent to precipitation [27,28]. Our previous investigation of L-PLA fractionation demonstrated no significant change in degree of crystallinity of L-PLA recovered from the GAS fractionation process (approximately 20% crystallinity) as a function of GAS process parameters [18].

#### 4. Conclusions

GAS fractionation complements existing polymer fractionation techniques using compressed or SCFs, while operating at mild temperatures and pressures [29]. GAS is a versatile fractionation technique capable of precipitating either high or low molecular weight fractions of semicrystalline L-PLA depending on choice of processing conditions. Our previous investigation has also demonstrated that multiple fractionation steps can be used to achieve a desired range of NMW [18], further supporting the versatility of this technique.

An ANOVA was used to determine the statistical significance of GAS variables on fractionation, and as a means to predict the conditions necessary to achieve a desired MW fraction. Through experimentation and statistical analysis, this work quantifies the importance of polymer concentration as a process variable, with pressurization rate and organic solution volume being of secondary significance. Thus, solution concentration, and not the traditional pressur-

ization rate, is identified as a primary variable to manipulate the fractionation of polymers via compressed antisolvent techniques. Stepwise fractionation has been demonstrated with GAS, suggesting the importance of quantifying the effect of polymer concentration on the resulting molecular weight of the processed polymer. While the influence of the processing variables has been demonstrated, there is a need for a more fundamental description of polymer fractionation as a function of GAS variables (including polymer concentration) that cannot be achieved with an ANOVA.

However, identifying the significant process variables provides a framework for additional fundamental studies regarding precipitation mechanisms in complex, non-equilibrium antisolvent processes. For example, the ability to precipitate both high and low MW PLA fractions suggests a change in the demixing mechanism in the semicrystalline polymer, which is primarily dependent on polymer concentration under the isothermal processing conditions investigated in this work. Examining such demixing events with in situ light scattering techniques, such as those used to study pressure induced phase separation [21], would provide direct evidence of the demixing mechanism as a function of composition and temperature.

#### Acknowledgements

The authors would like to thank Patrick DeLuca and Sisay Gebrekidan of the University of Kentucky's School of Pharmacy for providing an analytical procedure for determining the molecular weight of PLA.

#### References

- [1] McHugh M, Krukonis V. *Supercritical fluid extraction: principles and practice*. 2nd ed. Stoneman, MA: Butterworth/Heinemann, 1994.
- [2] Knutson BL, Debenedetti PG, Tom JW. In: Cohen H, Bernstein H, editors. *Drugs and pharmaceutical science*, vol. 77. New York: Marcel Dekker, 1996. Chapter 3.
- [3] Reverchon E. J *Supercrit Fluids* 1999;15:1–21.
- [4] Gallager PM, Coffey MP, Krukonis VJ, Klasutis N. Gas antisolvent recrystallization: new process to recrystallize compounds insoluble in SCF. In: Johnston KP, Penninger JML, editors. *Supercritical fluid science and technology*, ACS Symposium Series no., 406. Washington, DC: ACS, 1989. Chapter 2.
- [5] Dixon DJ. PhD Thesis. University of Texas, Austin; 1992.
- [6] Dixon DJ, Johnston KP, Bodemeier RA. *AIChE J* 1993;39(1):127–39.
- [7] Randolph TW, Randolph AD, Mebes M, Yeung S. *Biotechnol Prog* 1993;9(4):429–35.
- [8] Amaro-González D, Mabe G, Zabaloy M, Brignole EA. *J Supercrit Fluids* 2000;17:249–58.
- [9] Dixon DJ, Johnston KP. *AIChE J* 1991;37(10):1441–9.
- [10] Berends EM, Bruinsma OSL, de Graauw J, van Rosmalen GM. *AIChE J* 1996;42:431–9.
- [11] Bertucco A, Lora M, Kikic I. *AIChE J* 1998;44(10):2149–58.
- [12] Tan C, Lin H. *Ind Engng Chem Res* 1999;38:3898–902.
- [13] Muller M, Meier U, Kessler A, Mazzotti M. *Ind Engng Chem Res* 2000;39:2260–8.

- [14] Winters MA, Frankel DZ, Debenedetti PG, Carey J, Devaney M, Przybycien TM. *Biotechnol Bioeng* 1999;62(3):247–58.
- [15] Thiering R, Dehghani F, Foster N. *Proceedings of the International Symposium on Supercritical Fluids*, Atlanta, GA; 2000.
- [16] Catchpole OJ, Hochmann S, Anderson SRJ. *Proceedings of the International Symposium on High Pressure*, Zurich; 1996.
- [17] Tan C, Chang W. *Ind Engng Chem Res* 1998;37:1821–6.
- [18] White K. MS Thesis. University of Kentucky, Lexington; 1997.
- [19] Bulte AMW, Folkers B, Mulder MHV, Smolders CA. *J Appl Polym Sci* 1993;50:13–26.
- [20] Van de Witte P, Dijkstra PJ, Van den Berg JWA, Feijen J. *J Polym Sci, B: Polym Phys* 1997;35:763–70.
- [21] Liu K, Kiran E. *J Supercrit Fluids* 1990;16:60.
- [22] Jalil R, Nixon JR. *J Microencapsul* 1990;7(1):53–66.
- [23] Kim JH, Paxton TE, Tomasko DL. *Biotechnol Prog* 1996;12:650–61.
- [24] Billmeyer FW. *Textbook of polymer science*. New York: Wiley, 1984.
- [25] Box GEP, Hunter WG, Hunter JS. *Statistics for experiments: an introduction to design, data analysis, and model building*. New York: Wiley, 1991.
- [26] Bulte AMW, Naafs EM, van Eeten F, Mulder MHV, Smolders CA. *Polym J* 1996;37(9):1647–55.
- [27] Lambert SM, Paulaitis ME. *J Supercrit Fluids* 1991;4(15):15–23.
- [28] Zhang Z, Handa YP. *Macromolecules* 1997;26:8505–7.
- [29] Bungert B, Sadowski G, Arlt W. *Ind Engng Chem Res* 1998;37:3208–20.